Butler, M. R. G., Armour, S. M. D., Fletcher, P. N., Nix, A. R., & Bull, D. R. (2001). Viterbi decoding strategies for 5 GHz wireless LAN systems. IEEE 54th Vehicular Technology Conference, 2001 (VTC 2001-Fall), 1, 77 - 81. 10.1109/VTC.2001.956559

Viterbi Decoding Strategies for 5 GHz Wireless LAN Systems

M.R.G. Butler, S. Armour, P.N. Fletcher, A.R. Nix, D.R. Bull
Centre for Communications Research, University of Bristol, UK.
E-mail: *mike.butler@bristol.ac.uk*

Abstract— **Standards for the operation of Wireless Local Area Network (WLAN) technology in the 5 GHz band have been developed in Europe, North America and Japan. These systems employ Orthogonal Frequency Division Multiplexing (OFDM) technology, and utilize Forward Error Correction (FEC) coding, based on a 1/2-rate convolutional encoder, to combat frequency selective fading caused by multipath channels.**

This paper examines methods, based on the popular Viterbi algorithm, for Maximum-Likelihood (ML) decoding of this convolutional code within the WLAN baseband receiver. Although the paper focuses on the European HIPERLAN/2 standard, because of international Physical (PHY) layer harmonization, the work is equally applicable to the North American and Japanese WLAN systems.

Received error rate results, based on a software simulation of the HIPERLAN/2 PHY layer, are presented for both hard and soft decision decoding strategies. In addition, the effect of quantization on soft decision decoding is investigated. The results highlight the importance of the decoder design on the performance of the WLAN.

I. Introduction

NEW high speed Wireless Local Area Network (WLAN) technology standards exist in Europe (ETSI HIPERLAN/2), North America (IEEE 802.11a) and Japan (MMAC HISWANa) [1]. These WLAN systems will facilitate wireless connection of electronic devices at bit rates up to 54 Mbit/s. Co-operation between the three standardization bodies has ensured that the Physical (PHY) layers of the three standards, which handle over-air data transport functions, are harmonized to a large extent. They are all based on Orthogonal Frequency Division Multiplexing (OFDM) and, in order to combat fading of OFDM subcarriers caused by frequency selective channels, they employ similar Forward Error Correction (FEC) coding to transmitted bit streams. This FEC coding is based on an industry-standard 1/2-rate convolutional code.

Effective decoding of the convolutional code is an important aspect of the WLAN baseband receiver design. This paper investigates decoding methods, based on the widely-used Viterbi algorithm, that are compatible with the 5 GHz WLAN standards. The paper focuses on a model of the HIPERLAN/2 Physical (PHY) layer; however, because of the similarity of the PHY layers of HIPERLAN/2, IEEE 802.11a and MMAC HISWANa, the results are broadly valid for all three systems.

The paper is structured as follows: Section II outlines the HIPERLAN/2 PHY-layer software simulation used to obtain the performance results presented in the paper. It provides details of the FEC coding scheme and introduces notation with which the decoding algorithms that follow are described. Section III summarizes both hard and soft decision decoding strategies, and characterizes them in terms of received error rate. Finally, Section IV investigates the effect of quantization on the performance of soft decision decoding.

II. A HIPERLAN/2 PHY Layer Model

Fig. 1 shows a reference transmitter configuration for the HIPERLAN/2 PHY layer. User data for transmission is passed from the higher Data Link Control (DLC) protocol layer as a stream of 54-byte Protocol Data Units (PDUs)[1]. This sequence of bits is scrambled, FEC coded and interleaved. The bit stream is then divided into groups of 1, 2, 4 or 6 bits, which are mapped to Gray-coded constellation points. These constellation vectors characterize the symbols to be modulated onto the OFDM subcarriers. The subcarrier modulation scheme is determined by the transmission mode in use—the HIPERLAN/2 standard defines seven transmission modes each with a different modulation and FEC coding configuration, which are summarized in Table I. OFDM modulation is achieved using a 64-point inverse Fast Fourier Transform (FFT) process, and the complex baseband transmit signal is completed with the addition of cyclic guard intervals at the beginning of each OFDM frame, and a preamble at the beginning of the entire signal stream.

TABLE I
HIPERLAN/2 Transmission Modes.

Mode	Modulation	Coding Rate	Bit Rate (Mbit/s)
1	BPSK	1/2	6
2	BPSK	3/4	9
3	QPSK	1/2	12
4	QPSK	3/4	18
5	16-QAM	9/16	27
6	16-QAM	3/4	36
7	64-QAM	3/4	54

In Fig. 1, $\{T_{l,k}\}$ denotes the sequence of subcarrier constellation points, where k indexes the subcarrier that the symbol is transmitted on and l is the OFDM frame of which the subcarrier is a part. Since, within each OFDM frame, 48 subcarriers carry data $k = 0 \ldots K = 47$; the total number of frames within a particular transmission

[1]9-byte PDUs are also specified, but these are used exclusively for control information.

0-7803-7005-8/01/$10.00 (c) 2001 IEEE

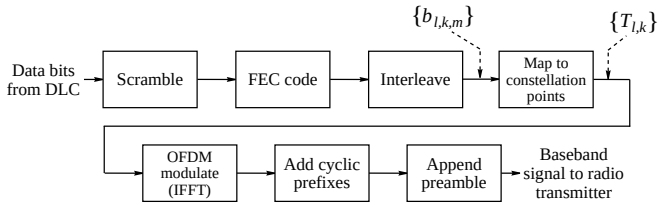

Fig. 1. HIPERLAN/2 transmitter reference configuration.

burst, L where $l = 0 \ldots L-1$, is a function of the length of the PDU train passed from the DLC and the transmission mode in use. The sequence of bits after scrambling, coding and interleaving is denoted $\{b_{l,k,m}\}$. Here, the subscript m indexes the bit within the symbol to which it is mapped; the number of bits per symbol is M. As this implies, the mapping process converts a steam of $L \times K \times M$ bits to $L \times K$ complex constellation vectors.

Fig. 2 provides detail of the FEC encoding process. The coding for all transmission modes is based on the same 1/2-rate, constraint length 7, mother convolutional code, described by generator polynomials $G_1 = 133_8$ and $G_2 = 171_8$. The higher coding rates are obtained by puncturing, or removing bits from, the basic 1/2-rate coded bit stream. Fig. 3 shows a schematic diagram for the mother code. To ensure that the convolutional encoder finishes in the all-zero state, 6 zero bits are appended to the input bit stream prior to the 1/2-rate encoding. After this initial coding, two stages of puncturing are performed. The first stage of puncturing (P1) removes 12 bits from the output stream. The removal of these output bits accounts for the 6 tail bits added to the input bit stream. The second stage of puncturing (P2) removes bits, according to a regular puncturing pattern, in order to achieve the coding rate required for the transmission mode in use.

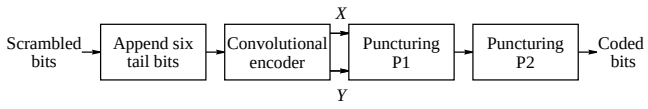

Fig. 2. Detail of FEC coding block.

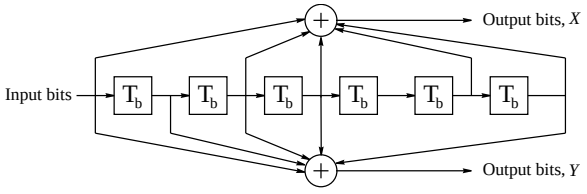

Fig. 3. Convolutional encoder schematic.

In order to simulate the process of radio transmission, the software simulation utilizes a model of the multipath channel. During the standardization of HIPERLAN/2, ETSI developed a number of channel profiles for simulating the radio link [2]. The results given in this paper are based on channel model 'A', which represents a typical indoor office environment with non-line of sight conditions and 50 ns average root mean squared (rms) delay spread. This is a delay-line channel model with a near-exponential power delay profile and 18 statistically independent Rayleigh distributed taps.

Fig. 4 illustrates a reference HIPERLAN/2 receiver configuration. The signal from the radio receiver is sampled at 50 ns intervals. The samples that represent the cyclic guard intervals are then removed and OFDM demodulation is achieved with the FFT operation. After OFDM demodulation, the preamble section of the received signal is used to form an estimate of the transmission channel, $\{H_k\}$—commonly termed the Channel State Information (CSI)—whilst the data part of the signal forms a sequence of received vectors, $\{R_{l,k}\}$. These are equalized by the CSI in order to compensate for the narrowband subcarrier distortion caused by the channel; the sequence of received symbol vectors that result are denoted $\{T'_{l,k}\}$. This process of frequency domain equalization normalizes the magnitude of each $T'_{l,k}$ and ensures that they are phase-aligned. The subsequent de-mapping converts $\{T'_{l,k}\}$ to either $\{d^{\text{hard}}_{l,k,m}\}$ or $\{d^{\text{soft}}_{l,k,m}\}$, dependent on whether the decoding strategy is hard or soft decision. De-interleaving then produces $\{x^{\text{hard}}_{l,k,m}\}$ or $\{x^{\text{soft}}_{l,k,m}\}$, which form the input to the Viterbi decoder. Dependent on the decoding strategy the CSI may also be input to the decoding stage. The Viterbi decoder outputs a sequence of bits which, after de-scrambling, form the received bit stream passed to the DLC layer.

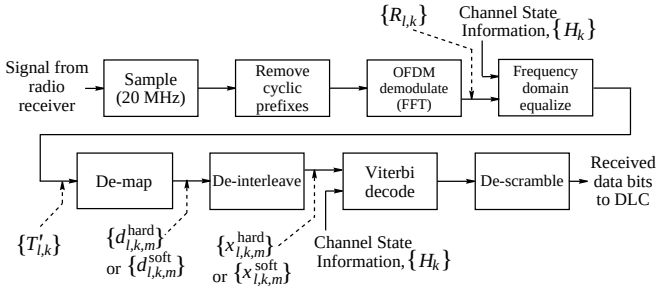

Fig. 4. HIPERLAN/2 reference receiver.

III. Viterbi Decoding Strategies

The Viterbi algorithm [3][4] is a widely-used method of decoding convolutional codes. It is an efficient implementation of the Maximum-Likelihood (ML) detector: the algorithm searches the possible codewords of the convolutional code and detects the one that is most likely to have generated the received sequence. The search procedure steps through the code trellis, and for each path through the trellis computes a metric which quantifies the discrepancy between the received sequence and the possible coded sequence. A history is maintained of the paths through the trellis that have minimum metrics associated with them. By taking advantage of the structure of the convolutional code, the Viterbi algorithm avoids the need to consider every possible coded sequence and thus greatly reduces the effort required for ML decoding.

The 1/2-rate mother convolutional code used within the 5 GHz WLAN standards is described by a 64-state trellis and decoding is based on this trellis irrespective of the coding rate. Punctured bits, discarded at the transmitter, are replaced by dummy bits, inserted into the received bit stream. These dummy bits are marked so that they do not contribute to the calculation of the path metrics.

The decoding strategies considered here are all based on the same search routine. What differs in each case is the method for computing the path metrics. As mentioned in the previous section, the decoding strategy in use determines the operation of the de-mapping process, which converts the $L \times K$ received symbol vectors $\{T'_{l,k}\}$ to a $L \times K \times M$ sequence $\{d^{\text{hard}}_{l,k,m}\}$ or $\{d^{\text{soft}}_{l,k,m}\}$. Hence, for each decoding strategy, in addition to the path metric calculation, the de-mapping mechanism is also described.

A. Hard Decision Decoding

With hard decision decoding, the Viterbi algorithm searches for the path though the trellis whose codeword differs in the least number of bits from the hard-limited received sequence. The de-mapping process involves identifying the nearest Gray-coded constellation point to each received subcarrier symbol vector, $T'_{l,k}$, and the resulting $d^{hard}_{l,k,m} \in \{0,1\}$ and $x^{hard}_{l,k,m} \in \{0,1\}$. The Viterbi decoder then detects the code sequence that minimizes the Hamming distance

$$\sum_{l=0}^{L-1} \sum_{k=0}^{K-1} \sum_{m=0}^{M-1} |c_{l,k,m} - x^{\text{hard}}_{l,k,m}| \qquad (1)$$

where $\{c_{l,k,m}\}$ denotes the binary codeword associated with a particular path through the trellis, and the minimization is over all possible codewords.

For BPSK and QPSK modulated subcarriers, hard decision de-mapping is straightforward. With BPSK modulation, each received symbol maps to a single bit, and the detected bit is determined by the sign of the in-phase (I) signal component. Similarly, with QPSK modulation each received symbol maps to 2 bits, which are determined by the sign of the in-phase and quadrature (Q) signal components. For 16-QAM and 64-QAM modulation, the decision method is more complicated and more 'decision boundaries', that define the points at which the polarity of the de-mapped bits change, are introduced. Fig. 5 shows the decision boundaries (labelled B1, B2, B3 and B4) for 16-QAM modulation. De-mapping for 64-QAM modulation involves a further level of decision boundaries.

Fig. 6 shows the PDU Error Rate (PER) performance of the seven HIPERLAN/2 PHY layer transmission modes with hard decision Viterbi decoding. PER is plotted against the 'Carrier-to-Noise ratio', C/N, which is the ratio of the average received power per subcarrier to the average power of the AWGN added at the receiver.

B. Soft Decision Decoding

If a soft decision decoding strategy is employed, the de-mapping process no longer makes a hard decision based on the received constellation vectors. Instead, $\{T'_{l,k}\}$ is de-mapped to $\{d^{\text{soft}}_{l,k,m}\}$, a sequence of signed one-dimensional distance values. Fig. 7 shows an example of the soft de-mapping process for 16-QAM modulation. The magnitude of each $d^{\text{soft}}_{l,k,m}$ is the distance of $T'_{l,k}$ normal to the appropriate decision boundary. The sign of $d^{\text{soft}}_{l,k,m}$ indicates the polarity of the de-mapped bit, and is determined by which side of the relevant decision boundary $T'_{l,k}$ lies.

Following this de-mapping and the subsequent de-interleaving, the sequence $\{x^{\text{soft}}_{l,k,m}\}$ characterizes the confidence associated with the polarity of each received bit. A standard approach to soft decision decoding would be for the Viterbi algorithm to search for the path through the code trellis that has maximum overall confidence

$$\sum_{l=0}^{L-1} \sum_{k=0}^{K-1} \sum_{m=0}^{M-1} c^{\text{nrz}}_{l,k,m} x^{\text{soft}}_{l,k,m} \qquad (2)$$

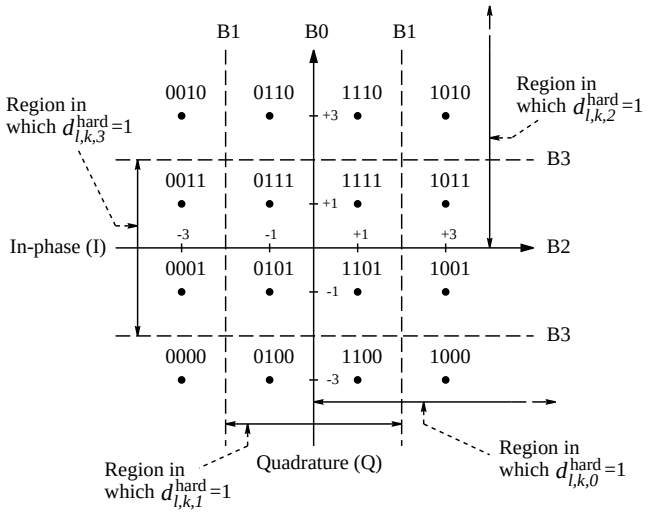

Fig. 5. Constellation for 16-QAM modulation showing hard decision de-mapping and decision boundaries.

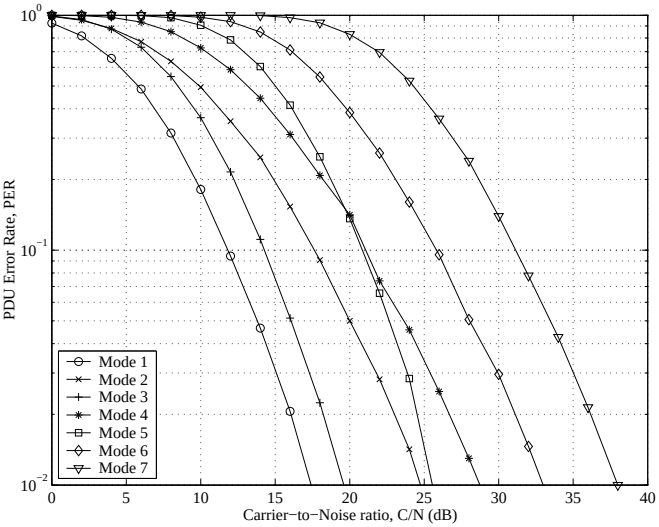

Fig. 6. PER against C/N for all HIPERLAN/2 modes with hard decision Viterbi decoding.

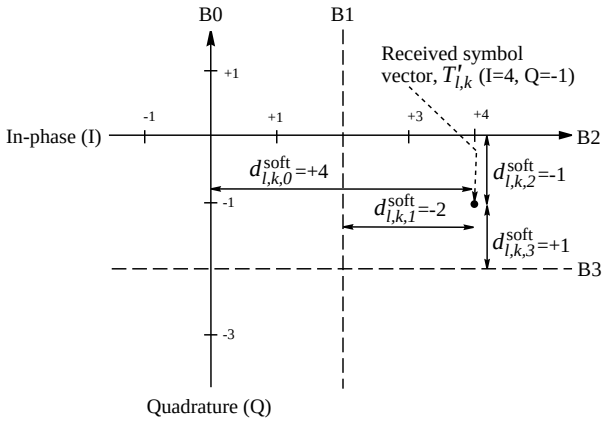

Fig. 7. Example de-mapping of a received vector to signed one-dimensional distance values for 16-QAM modulation.

where $\{c^{\text{nrz}}_{l,k,m}\}$ indicates a nonreturn-to-zero representation of the codewords. However, because of the availability of information about the channel at the receiver, a better method is to weight the path metrics by the magnitude of the CSI (this is referred to as 'soft CSI decision decoding'). The Viterbi algorithm then finds the path that maximizes:

$$\sum_{l=0}^{L-1}\sum_{k=0}^{K-1}\sum_{m=0}^{M-1}|H_k|^2 c^{\text{nrz}}_{l,k,m}x^{\text{soft}}_{l,k,m} \tag{3}$$

The effect of weighting the metrics by the CSI is that elements of $\{x^{\text{soft}}_{l,k,m}\}$ transmitted on subcarriers that experienced a high level of attenuation due to the channel contribute less to the metric calculation than elements of $\{x^{\text{soft}}_{l,k,m}\}$ carried on less attenuated subcarriers. This means that a small weighting is applied to information from subcarriers with low reliability and a higher weighting is applied to information from higher-reliability subcarriers. The importance of weighting the path metrics by the CSI has been highlighted in [5], [6] and [7].

Fig. 8 compares the PER performance of HIPERLAN/2 mode 5 with hard decision decoding, standard soft decision decoding and soft CSI decision decoding. The results clearly indicate the importance of the use of the CSI in the branch metric calculation. The performance of soft decision decoding is very poor—in order to achieve a PER of 10^{-2}, the C/N requirement is more than 8 dB higher than with hard decision decoding; soft CSI decision decoding outperforms hard decision decoding by a further 5 dB. Standard soft decision decoding performs poorly because of the noise amplifying effect of the frequency domain equalization process: noise on highly attenuated subcarriers is enhanced significantly when the received symbol magnitudes are normalized. Path metric calculations in the Viterbi decoder can be severely affected by this noise. Hard decision decoding provides improved performance because the negative effect of the amplified noise on the path metrics is limited by the hard de-mapping process. Soft decision decoding weighted by the CSI counteracts the high degree of noise on faded subcarriers by assigning them a small weighting in the path metric calculation.

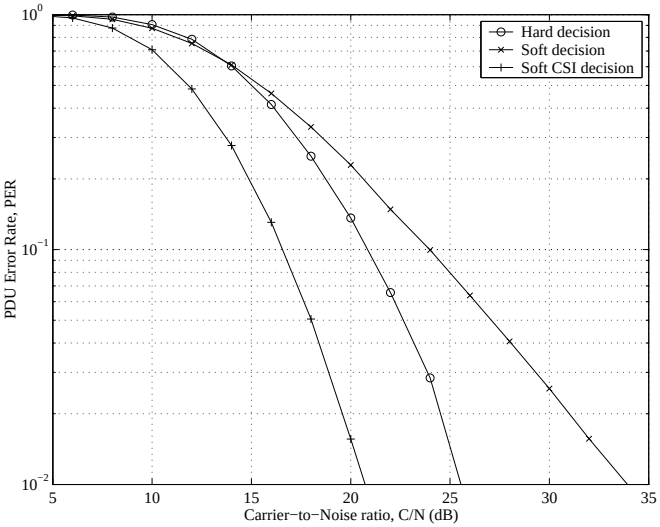

Fig. 8. PER against C/N for HIPERLAN/2 mode 5 with hard decision, soft decision and soft CSI decision Viterbi decoding strategies.

Fig. 9 indicates the PER versus C/N for the HIPERLAN/2 PHY layer transmission modes with soft CSI decision decoding. Compared to the hard decision results in Fig. 6, with the soft CSI strategy there is a marked improvement in performance. Indeed, in order to achieve a PER of 10^{-2}, the C/N requirement is reduced by between 4.7 and 9.3 dB. It is noticeable that the improved metric provided by soft CSI decision decoding has more benefit for modes utilizing less-powerful 3/4-rate coding—for the 3/4-rate modes (2,4,6 and 7) the improvement with soft CSI decoding is between 7.7 and 9.3 dB, whilst the gain for the other modes is between 4.7 and 6.7 dB.

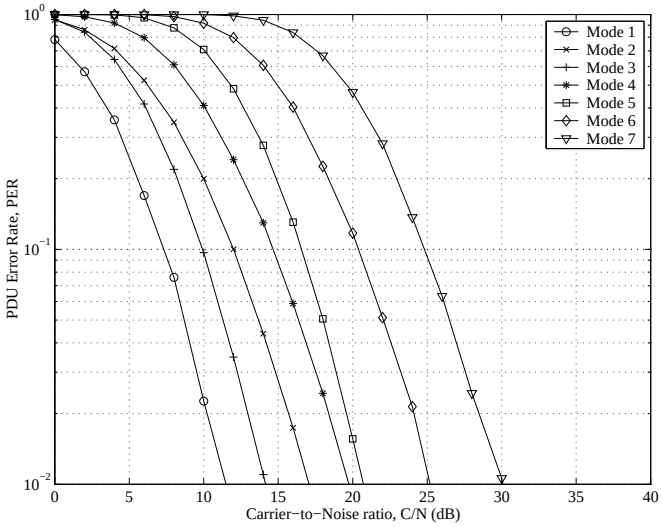

Fig. 9. PER against C/N for all HIPERLAN/2 modes and soft CSI decision Viterbi decoding.

The scale of the performance enhancement provided by soft CSI decision decoding could have a significant impact on the level of service and types of application supported by a WLAN system. For example, a WLAN modem operating

with soft CSI decoding, as opposed to hard decision decoding, could provide greater throughput to a given user, be able to support a larger number of users, or be capable of operating over a wider geographical area. However, these benefits must be traded-off against the increased complexity of the soft CSI decision strategy; the more complex the decoding strategy, the more processing power required to implement it.

IV. Soft metric quantization

The soft CSI decision results presented in the previous section were based on simulations that used floating point accuracy within the path metric calculations. In practical receivers, the level of accuracy will be limited to a small number of bits. Fig. 10 shows the structure of the soft CSI decision decoder when the input to the Viterbi decoder is quantized. The de-interleaved stream, $\{x^{\text{soft}}_{l,k,m}\}$, is first multiplied by the appropriate CSI magnitude in order to account for the weighting by $|H_k|^2$ in (3). The resulting sequence is then quantized according to a discrete number of threshold levels. Fig. 11 shows the quantization mapping for an 8-level (3-bit) implementation; this is the same quantization as used in [8].

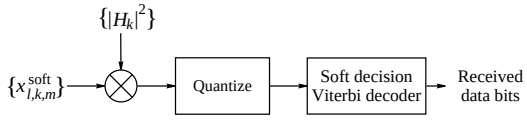

Fig. 10. Soft decision weighted by CSI decoder with quantization.

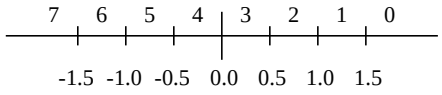

Fig. 11. 3-bit quantization thresholds and levels.

Fig. 12 plots the C/N required to achieve a PER of 10^{-2} with various levels of quantized soft CSI decision decoding for each of the HIPERLAN/2 transmission modes. For comparison, the results with a floating point implementation, and with hard decision decoding, are also shown. Again, there is a noticeable difference between the performance of the modes based on 3/4-rate coding, and those based on 1/2-rate or near-1/2-rate (9/16-rate) coding; the 3/4-rate coding is more sensitive to the effects of quantization. In order to achieve performance within 0.5 dB of the floating point implementation, the 3/4-rate coded modes require 6-bit accuracy, while the same level of performance can be achieved for the other modes with a 4-bit implementation.

V. Conclusions

Both hard and soft decision strategies for ML decoding within 5 GHz WLAN systems have been investigated. The results have highlighted that the decoding scheme implemented can have a significant impact on the expected performance of a WLAN. The importance of weighting path metrics by the CSI when soft decision decoding is employed has been emphasized. Soft CSI decision decoding with floating point accuracy has been shown to outperform hard decision decoding by between 4.7 and 9.3 dB. In addition it has been demonstrated that when the input to the soft decision decoder is quantized, in order to achieve performance within 0.5 dB of the floating point case for all transmission modes, 6-bit accuracy is required.

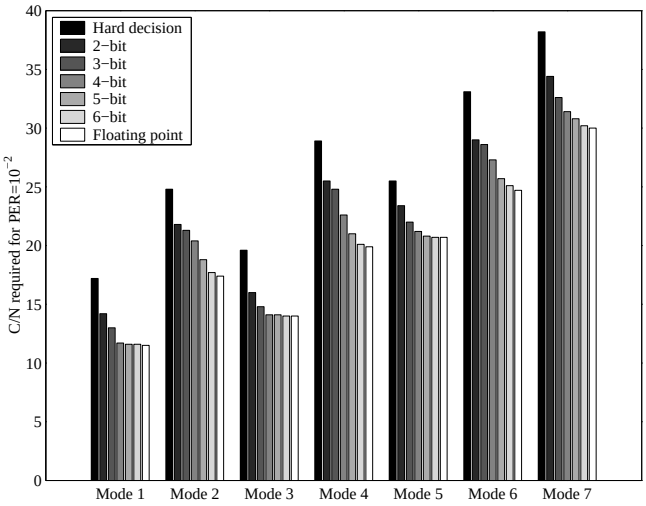

Fig. 12. C/N required to achieve a PER of 10^{-2} for all HIPERLAN/2 modes with hard decision decoding, soft CSI decision decoding with floating point accuracy, and levels of quantized soft CSI decision decoding.

Acknowledgments

Michael Butler gratefully acknowledges the financial assistance of Blue Wave Systems Ltd. and the Engineering and Physical Sciences Research Council. Simon Armour gratefully acknowledges the support of Toshiba Research Europe Ltd.

References

[1] R. Van Nee, "New high-rate wireless LAN standards," *IEEE Communications Magazine*, vol. 87, no. 12, pp. 82–22, December 1999.

[2] J. Medbo and P. Schramm, "Channel models for HIPERLAN/2 in different indoor scenarios," *ETSI document 3ERI085B*, March 1998.

[3] A. Viterbi, "Convolutional codes and their performance in communication systems," *IEEE Transactions on Communications*, vol. 19, no. 5, pp. 751–772, October 1971.

[4] G. Forney, "The Viterbi algorithm," *Proceedings of the IEEE*, vol. 61, no. 3, pp. 268–278, March 1973.

[5] H. Sari, G. Karam, and I. Jeanclaude, "Transmission techniques for digital terrestrial TV broadcasting," *IEEE Communications Magazine*, vol. 83, no. 2, pp. 100–109, February 1995.

[6] W. Lee, H. Park, and Park J., "Viterbi decoding method using channel state information in COFDM system," *IEEE Transactions on Consumer Electronics*, vol. 45, no. 3, pp. 533–537, August 1999.

[7] J. Stott, "Explaining some of the magic of COFDM," in *20th International Television Symposium*, Montreux, Switzerland, June 1997.

[8] J. Heller and I. Jacobs, "Viterbi decoding for satellite and space communication," *IEEE Transactions on Communications*, vol. 19, no. 5, pp. 835–848, October 1971.